NANO LETTERS

2008
Vol. 8, No. 2
668−672

Functionalization of Electrospun TiO_2 Nanofibers with Pt Nanoparticles and Nanowires for Catalytic Applications

Eric Formo,[†,§] Eric Lee,[†,§] Dean Campbell,[‡] and Younan Xia*[,†]

Department of Biomedical Engineering, Washington University, St. Louis, Missouri 63130, and Department of Chemistry and Biochemistry, Bradley University, Peoria, Illinois 61625

Received December 4, 2007; Revised Manuscript Received January 8, 2008

ABSTRACT

This paper reports a simple procedure for derivatizing the surface of anatase TiO_2 nanofibers with Pt nanoparticles and then Pt nanowires. The nanofibers were prepared in the form of a nonwoven mat by electrospinning with a solution containing both poly(vinyl pyrrolidone) and titanium tetraisopropoxide, followed by calcination in air at 510 °C. The fiber mat was then immersed in a polyol reduction bath to coat the surface of anatase fibers with Pt nanoparticles of 2–5 nm in size with controllable density of coverage. Furthermore, the coated fibers could serve as a three-dimensional scaffold upon which Pt nanowires of roughly 7 nm in diameter could be grown at a high density and with a length up to 125 nm. The fiber membranes functionalized with Pt nanoparticles and nanowires are interesting for a number of catalytic applications. It was found to show excellent catalytic activity for the hydrogenation of azo bonds in methyl red, which could be operated in a continuous mode by passing the dye solution through the membrane at a flow rate of 0.5 mL/s.

One of the important applications of noble metal nanoparticles is their use as heterogeneous catalysts for various oxidation and reduction reactions.[1] One metal in particular, platinum, has received considerable interest primarily due to its superb performance as an industrial catalyst for applications that range from methanol oxidation in fuel-cell technology to three-way automobile catalytic conversion and hydrogenation reactions.[2] There are a number of methods for preparing heterogeneous catalysts; typical examples include deposition of metal nanoparticles on a monolithic support via gas-phase decomposition, in situ growth of metal nanoparticles on colloidal particles or carbon nanotubes via solution-phase reduction, and immobilization of metal nanoparticles onto colloidal particles or electrospun fibers.[3,4] Despite all the advancement in heterogeneous catalyst preparation, there is still great interest in developing catalytic supports from stable and inert membranes made of ceramic fibers. When fabricated from an appropriate material, such a membrane can provide a high porosity and large surface area and even help prevent sintering and limit poisoning.

Fiber membranes have been shown to be very useful for heterogeneous catalysis.[4] Recently, the nonwoven materials have been proven to be efficient photocatalysts and shown to be useful as supports for catalytic metal nanoparticles.[5] For example, metal nanoparticles on polymeric and carbon fibers have been shown to improve a number of catalytic reactions including the hydrogenation of carbonyls and alkenes.[4,6] The fiber membranes are commonly prepared in the form of a nonwoven mat via electrospinning,[7] which offers a simple and versatile route to the large-scale production of fibers from a variety of materials. Deposition of metal nanoparticles onto the electrospun fibers can be performed using different techniques. A common method involves spinning a polymer solution mixed with a metal salt to yield a membrane of composite fibers. Subsequent heating of the membrane yields fibers decorated with metal nanoparticles.[4,6] Post-treatment of the membrane can also deposit metal nanoparticles on the surface of the fibers. Our group has previously demonstrated this by photoreducing the desired metal salt to directly deposit metal nanoparticles onto the surface of the fibers.[8] Such a post-treatment seems ideal for making catalytic fiber membranes as it should simplify the electrospinning process, allowing for a greater level of control for both the size and coverage of the nanoparticles. In the present work, we modify the post-treatment technique and develop a facile method for decorating the surface of anatase fibers in a nonwoven mat with Pt nanoparticles. We further demonstrate the catalytic capability of the as-prepared membranes for the hydrogenation of azo bonds in methyl red to amines. Additionally, we have demonstrated that the

* To whom correspondence should be addressed. E-mail: xia@biomed.wustl.edu.
[†] Washington University.
[‡] Bradley University.
[§] These two authors contributed equally to this work.

10.1021/nl073163v CCC: $40.75
Published on Web 01/19/2008

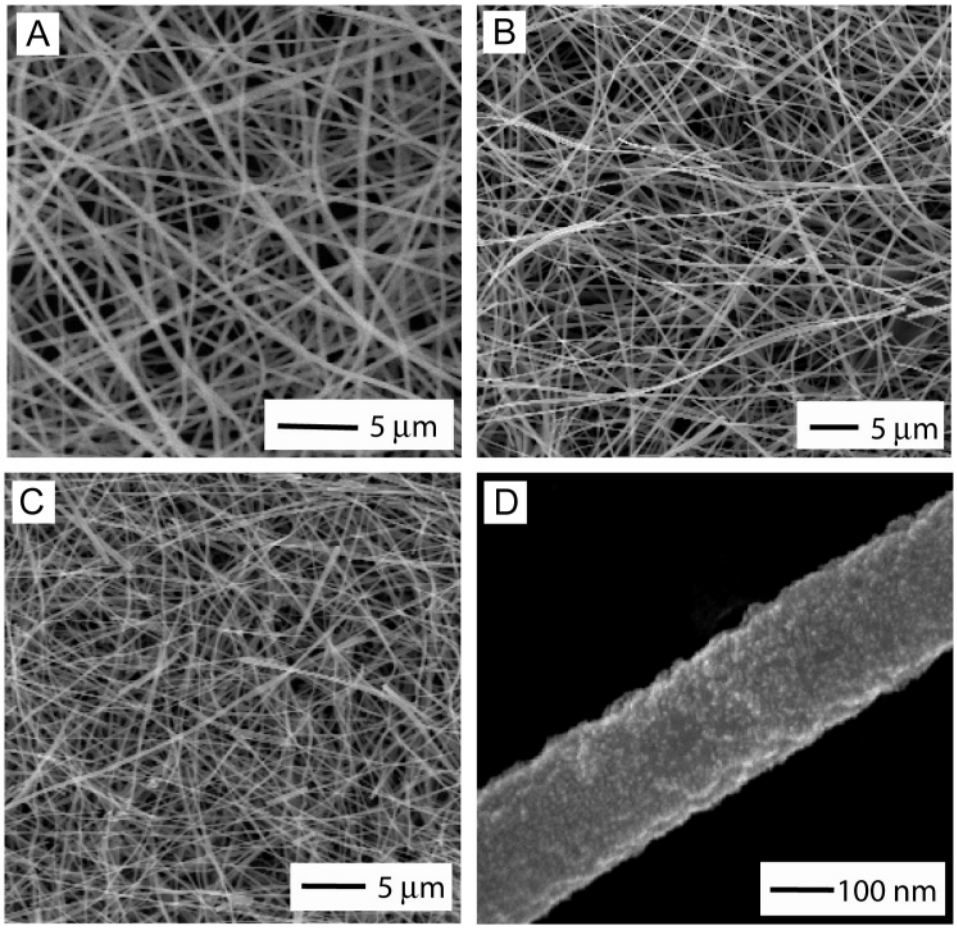

Figure 1. SEM images of (A) an as-spun, nonwoven mat of composite nanofibers composed of PVP and amorphous TiO_2; (B) a mat of anatase nanofibers prepared by calcining the sample in air at 510 °C for 6 h; (C) the anatase mat after the nanofiber surface had been decorated with Pt nanoparticles by immersing the sample in a polyol reduction bath for 7 h; and (D) a high-resolution SEM image of an individual fiber from the sample in (C).

nonwoven mat of TiO_2 fibers decorated with Pt nanoparticles could serve as a three-dimensional scaffold to generate Pt nanowires in an effort to further increase the active surface for catalysis.

We prepared nonwoven mats of anatase nanofibers using a protocol previously developed in our group, which involves electrospinning of a polymer solution mixed with a sol−gel precursor.[9] In the first step, we dissolved titanium tetraisopropoxide and poly(vinyl pyrrolidone) (PVP) in a mixture of ethanol and acetic acid and then electrospun the solution onto a grounded electrode. Figure 1A shows a scanning electron microscopy (SEM) image of an as-prepared nonwoven mat consisting of composite fibers made of PVP and amorphous TiO_2. After calcination in air at 510 °C for 6 h, the composite was converted into nanocrystalline anatase, together with a small amount of carbon residue arising from incomplete burning of the polymeric phase. As illustrated in Figure 1B, the nonwoven morphology was largely preserved during the calcination process while the diameter of the fibers was reduced from roughly 300 to 200 nm. It is worth pointing out that the high porosity of a typical nonwoven mat is advantageous for uniform deposition of Pt nanoparticles. Figure 1C shows an SEM image of the same membrane of anatase fibers after it had been immersed in an ethylene glycol (EG) solution containing a H_2PtCl_6 and PVP for 7 h, which resulted in the deposition of Pt nanoparticles on the surface of anatase nanofibers (see Figure 1D for an SEM image taken at a higher magnification). Again, there was essentially no change to the nonwoven morphology during the deposition of Pt nanoparticles.

Figure 2 demonstrates the ability to deposit Pt nanoparticles on the surface of nanofibers with varying densities by placing the anatase membrane in the polyol reduction bath for 3, 7, and 19 h, respectively. In the first step, the membrane of anatase fibers was immersed in EG and heated at 110 °C for 30 min to remove residual water in the system. As shown in Figure 2A, the anatase fiber had a relatively rough surface, which seems to be beneficial to the nucleation of Pt nanoparticles. In the next step, 1 mL of H_2PtCl_6 solution and 1 mL of PVP solution (both dissolved in EG) were added simultaneously over 1.5 min to the reaction solution. After 3 h of reaction, small Pt nanoparticles were observed on the fiber surface; these nanoparticles were about 2 nm in diameter and were evenly distributed across the entire surface of each fiber (Figure 2B). After the deposition of Pt nanoparticles, the membrane turned from white to dark gray and maintained this color past several washings with water.

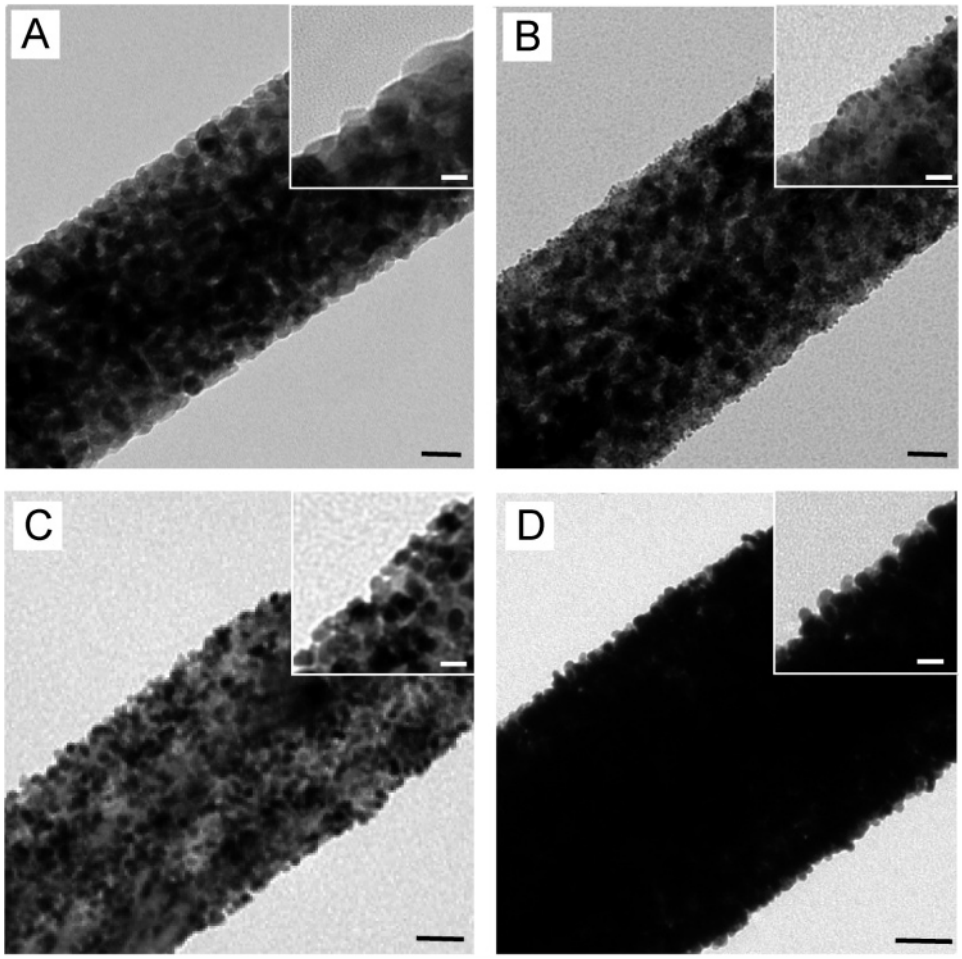

Figure 2. TEM images of (A) an individual anatase nanofiber taken from the nonwoven mat; and (B−D) nanofibers taken from the mat after it had been decorated with Pt nanoparticles by immersing the sample in the deposition bath for 3, 7, and 19 h, respectively. The scale bars are 50 nm, and the scale bars in the insets are 20 nm. Both the size and density of Pt nanoparticles increased with deposition time.

Once the reaction had progressed for 7 h, the density of Pt nanoparticles was further increased, along with an increase of their diameter to roughly 5 nm (Figure 2C). The last sample was prepared with a deposition time of 19 h. In this case, the surface of the fiber was completely covered by a sheath of densely packed Pt nanoparticles (Figure 2D). Energy dispersive spectroscopy analysis verifies that the amount of Pt nanoparticles being deposited on the anatase fibers is directly proportional to the reaction time, as the ratio of Pt to Ti increases from 0.71 to 0.99 and 1.4 when the deposition time was increased from 3 to 7 and 19 h, respectively (Supporting Information, Table S1).

It is possible to use the Pt nanoparticles deposited on anatase nanofibers as seeds to grow Pt nanowires.[10] Figure 3A shows a transmission electron microscopy (TEM) image of the edge of a anatase fiber after the sample had been coated with Pt nanoparticles. The decoration was achieved by placing the membrane in the polyol reduction bath for 19 h, as described previously. The high density of Pt nanoparticles gave us a scaffold upon which Pt nanowires could nucleate and then grow. To remove excess Pt nanoparticles that were not deposited on the fibers, the sample was washed several times with ethanol. After washing, the as-obtained membrane was placed again in a similar polyol solution containing a Pt salt and PVP. However, for the growth of Pt nanowires, a trace amount of $FeCl_3$ was added to serve as an oxidative etchant for Pt(0).[10] Once the growth of Pt nanowires was initiated, they could continually grow along the <111> direction until the supply of Pt(0) atoms was depleted. After growth of Pt nanowires, the fiber membrane became darker in color. As seen in Figure 3B, the Pt nanowires produced using this method ranged from 50 to 125 nm in length, which is longer than the wires produced in our previous work.[10] The increased length of the nanowires is advantageous, as the longer Pt nanowires will result in an increase in the catalytically active surface area. The diameter of these nanowires was determined to be on the order of 7 nm, which corresponds to previously reported values. Figure 3C shows that the entire surface of the anatase nanofiber was decorated with Pt nanowires. Figure 3D shows a high-resolution TEM image of a single Pt nanowire released from the surface of anatase nanofibers. The fringe spacing of 0.23 nm corresponds to the interplanar separation between the {111} planes, indicating that the growth direction of the nanowire was along the <111> axes.

To test the catalytic activity of the anatase fiber membranes decorated with Pt nanostructures, we have chosen to study the hydrogenation of the azo bond, which is present in many

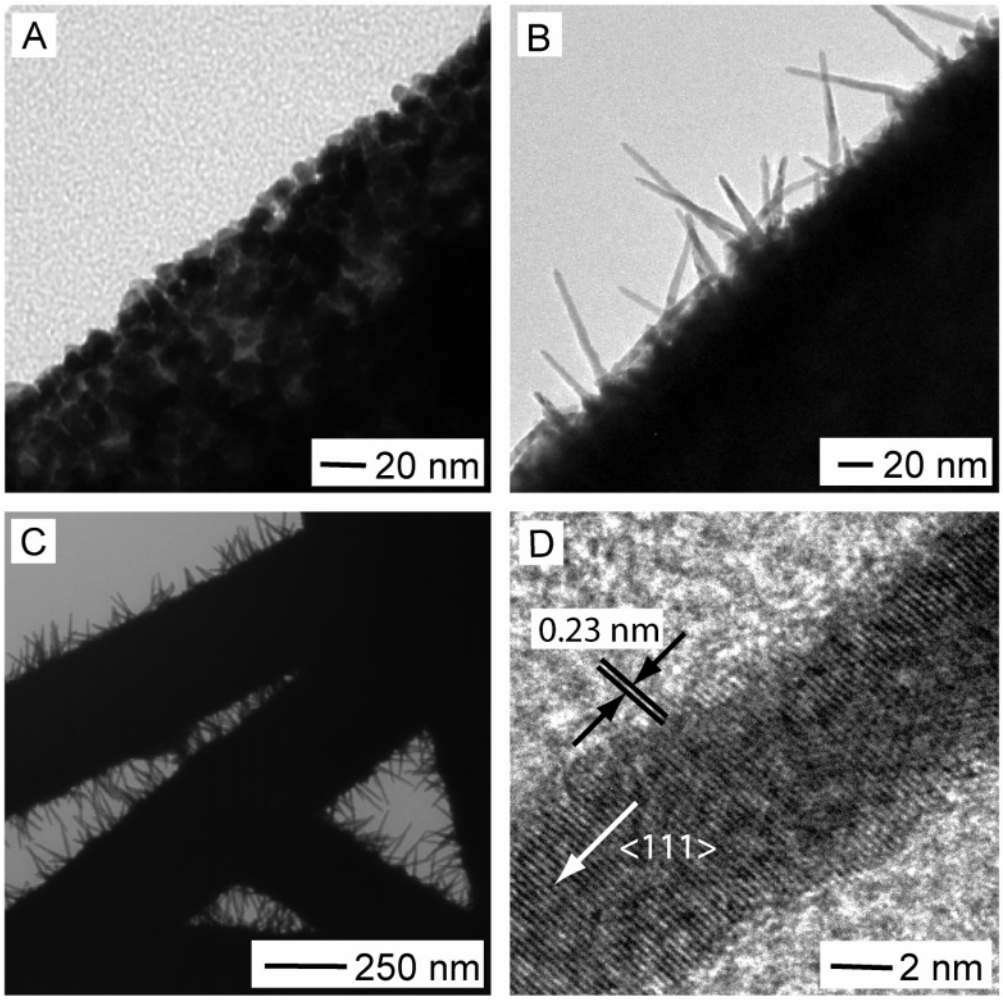

Figure 3. TEM images of (A) the edge of an anatase nanofiber after it had been decorated with Pt nanoparticles by immersing the sample in the deposition bath for 19 h; (B) the same sample after the surface had been decorated with Pt nanoparticles, followed by growth of Pt nanowires in another polyol reduction bath for 13.5 h; (C) the same sample as in (B), but at a lower magnification; and (D) high-resolution TEM image of an individual Pt nanowire removed from the nanofiber surface.

organic dyes. Methyl red serves as a good model compound to evaluate the catalytic activity of the Pt-coated membrane; cleavage of the azo bond takes place during hydrogenation of methyl red (see Supporting Information, Figure S1 for a schematic). The azo cleavage breaks the π-conjugation of the molecule and thus results in a color transformation from red to clear, which allows one to quantitatively measure and monitor the catalytic performance of the Pt-decorated fiber membrane by taking UV−vis spectra from a methyl red solution after passing through the membrane (Supporting Information, Figure S1). Specifically, we can focus on changes in UV−vis absorbance in the range of 500 to 575 nm.

The catalytic activity of fibers decorated with Pt nanoparticles and Pt nanowires can be seen in the UV−vis spectra taken from solutions of methyl red after hydrogenation (Figure 4). The highly porous nature of the fiber membrane allowed the methyl red solution to be passed through at a rate as high as 0.5 mL/s. In Figure 4 panels A and B, the top curves were taken from the untreated methyl red solution (46 μM in ethanol/water), showing broad peaks from 500 to 575 nm with an absorbance of 0.503 at 525 nm. After the methyl red solution had been saturated with H_2 gas and passed through the Pt-decorated fiber membranes, a sharp reduction in the absorbance was noted, indicating that the methyl red solution had been catalytically hydrogenated. Figure 4A compares the performance of membranes coated with Pt nanoparticles (at 3, 7, and 19 h) and Pt nanowires. The UV−vis spectra indicate that the lowest reduction of absorbance occurred with the fiber membrane coated with Pt nanoparticles at 3 h with a measured absorbance of 0.0933 at 525 nm. The absorbance at 525 nm was further reduced to 0.0436 and 0.0133 for the 7 and 19 h samples, respectively. This trend shows that the catalytic activities correlated with the length of time for Pt nanoparticle deposition with the 3 h sample having the lowest activity and the 19 h sample having the highest activity. This difference in catalytic activity was mainly caused by the varying densities of Pt nanoparticles on the membrane; as the density increases, there are more active sites for catalysis. The greatest reduction of absorbance occurred with the Pt nanowire-decorated membrane, which had a measured absorbance of 0.0044 at 525 nm. This is because the growth of Pt nanowires on the fiber further enlarges the active surface area, resulting

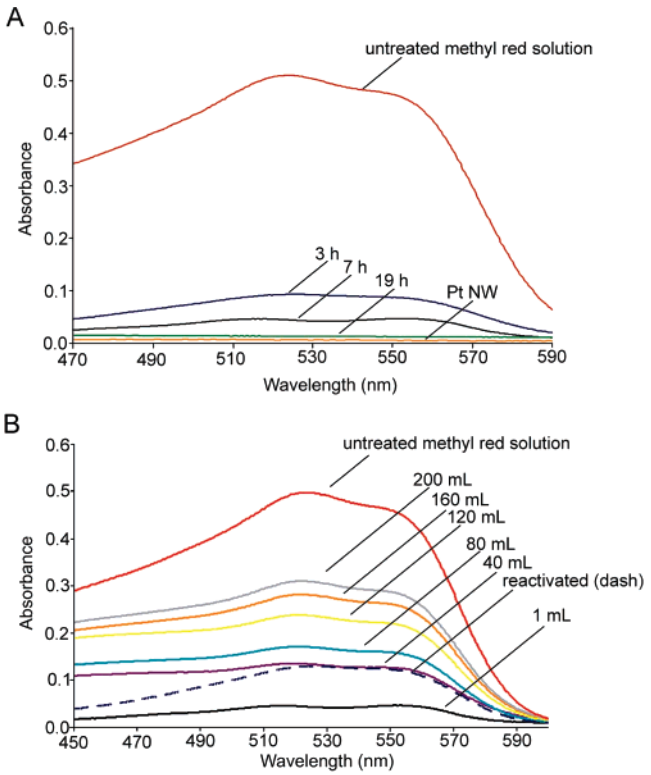

Figure 4. Azo bond cleavage of methyl red via hydrogenation using the decorated fiber membranes. (A) Reduction of UV−vis spectra peak intensity from a 46 μm methyl red solution before and after passing through the anatase membranes that had been decorated for 3, 7, and 19 h with Pt nanoparticles or with Pt nanowires. (B) After a gradual increase in the UV−vis peak intensity as more methyl red solution was passed through the anatase membrane that had been decorated with Pt nanoparticles for 7h, poisoning of the catalytic Pt occurred; spectra were taken in increments of 40 mL. Partial reactivation of the membrane was achieved by cleaning with 4 M nitric acid. The absorbance of the methyl red solution after passing through the reactivated membrane is represented by the dashed line.

in more efficient cleavage of the azo bond and a decrease in absorbance for the dye solution.

As more methyl red solution passed through the catalytic membrane, the supported Pt catalyst began to lose its activity (probably due to poisoning). The UV−vis spectra in Figure 4B shows that passing 1 mL of methyl red solution through the membrane resulted in a significant reduction of absorbance. However, as the total volume of methyl red solution passed through the membrane increased to 200 mL, the absorbance at 525 nm gradually increased as well. The poisoning effect could be partially reversed by passing 1 mL of nitric acid (4 M) through the system. After reactivating the membrane, passing 1 mL of the methyl red solution through the membrane resulted in a substantial reduction of absorbance, albeit the decrease was not as significant as the freshly prepared membrane.

In summary, we have demonstrated that we could decorate the surface of anatase nanofibers with Pt nanoparticles 2−5 nm in size using a simple chemical reduction process. The density of the Pt nanoparticles increased proportionally with the duration of deposition. The Pt nanoparticles coated on anatase nanofibers could also serve as seeds for the growth of Pt nanowires up to 125 nm in length. The resultant fiber membranes proved to have excellent catalytic activities for the hydrogenation of methyl red, and the efficiency kept improving as the coverage of the Pt nanoparticle increased. The methodology described in this report offers a simple and straightforward route to the immobilization of noble-metal nanocatalysts on fibrous supports using chemical reduction.

Acknowledgment. This work was supported in part by the NSF (DMR-0451788) and a gift from the I'NEST program of Philip Morris U.S.A. Y.X. is a Camille Dreyfus Teacher Scholar (2002−2007).

Supporting Information Available: Experimental section. This material is available free of charge via the Internet at http://pubs.acs.org.

References

(1) (a) Guliants, V. V. *Catal. Today* **2001**, *67*, 307. (b) Mizuno, N.; Misono, M. *Chem. Rev.* **1998**, *98*, 199. (c) Holderich, W. F.; Heitmann, G. *Catal. Today* **1997**, *38*, 227. (d) Hutching, G. J.; Derounane, E. G. *J. Mol. Catal. A: Chem.* **2004**, *5*, 220.

(2) (a) Chen, W.; Kim, J. L.; Sun, S.; Chen. S. *Phys. Chem. Chem. Phys.* **2006**, *8*, 2779. (b) Jun, C. H.; Park, Y. J.; Yeon, Y. R.; Choi, J. R.; Lee, W.; Ko, S. J.; Cheon, J. *Chem. Commun.* **2006**, 1619. (c) Song, H.; Riox, R. M.; Hoefelmeyer, J. D.; Komor, R.; Niesz, K.; Grass, M.; Yang P. D.; Somorjai, G. A. *J. Am. Chem. Soc.* **2006**, *128*, 3027. (d) Yan, W.; Mahurin, S. M.; Pan, Z.; Overbury, S. H.; Dai, S. *J. Am. Chem. Soc.* **2005**, *127*, 10480.

(3) (a) Yang, L. R.; Mayr, M.; Kurst, K.; Buchmeiser, M. R. *Chem.—Eur. J.* **2004**, *10*, 5761. (b) Wai. C. M.; Yoon. B. *J. Am. Chem. Soc.* **2005**, *127*, 17174. (c) Chien, C. C.; Jeng, K. T. *Mater. Chem. Phys.* **2006**, *99*, 80. (d) Gopidas, K. R.; Whitesell, J. K.; Fox, M. *Nano Lett.* **2003**, *3*, 1757. (e) Lu, Z.; Liu, G.; Phillips, H.; Hill, J.; Chang, J.; Kydd, R. *Nano Lett.* **2001**, *1*, 683.

(4) Graeser, M.; Pippel, E.; Greiner, A.; Wendroff, J. *Macromolecules* **2007**, *40*, 6032.

(5) (a) Zhan, S.; Chen, D.; Jiao, X.; Song, Y. *Chem. Commun.* **2007**, *20*, 2043. (b) Jin, M.; Zhang, X.; Emeline, A.; Liu, Z.; Tryk, D.; Murakami, T.; Fujishima, A. *Chem. Commun.* **2006**, *43*, 4483.

(6) (a) Wu, H.; Zhang, R.; Liu, X.; Lin, D.; Pan, W. *Chem. Mater.* **2007**, *19*, 3506. (b) Demir, M. M.; Gulgen, M. A.; Menceloglu, Y.; Erman, B.; Abramchuk. S. S.; Makhaeva E. E.; Khokhlov, A. R.; Matveeva, V. G.; Sulman, M. G. *Macromolecules* **2004**, *37*, 1787. (c) Patel, A.; Li, S.; Wang, C.; Zhang, W.; Wei, Y. *Chem. Mater.* **2007**, *19*, 1231.

(7) Li, D.; Xia, Y. *Adv. Mater.* **2004**, *16*, 1151.

(8) Li, D.; McCann, J.; Gratt, M.; Xia, Y. *Chem. Phys. Lett.* **2004**, *394*, 387.

(9) Li, D.; Xia, Y. *Nano Lett.* **2003**, *3*, 555.

(10) (a) Chen, J.; Xiong, Y.; Yin, Y.; Xia, Y. *Small* **2006**, *2*, 1399. (b) Lee, E. P.; Chen, J.; Yin, Y.; Campbell, C. T.; Xia, Y. *Adv. Mater.* **2006**, *18*, 3271. (c) Chen, J.; Herricks, T.; Geissier, M.; Xia, Y. *J. Am. Chem. Soc.* **2004**, *126*, 10854. (d) Lee, E. P.; Peng, Z.; Cate, D.; Yang, H.; Campbell, C. T.; Xia, Y. *J. Am. Chem. Soc.* **2007**, *129*, 10634.

NL073163V